HHS Public Access

Author manuscript

Biotechnol Bioeng. Author manuscript; available in PMC 2020 June 01.

Published in final edited form as:

Biotechnol Bioeng. 2019 June ; 116(6): 1523–1536. doi:10.1002/bit.26957.

A comparison of hMSC osteogenesis in PEG hydrogels as a function of MMP-sensitive crosslinker and crosslink density in chemically-defined medium

Aaron H. Aziz[1,2], **Stephanie J. Bryant**[1,2,3,*]

[1]Department of Chemical and Biological Engineering, 3415 Colorado Ave, University of Colorado, Boulder, CO 80309-0596

[2]BioFrontiers Institute, 3415 Colorado Ave, University of Colorado, Boulder, CO 80309-0596

[3]Material Science and Engineering, 3415 Colorado Ave, University of Colorado, Boulder, CO 80309-0596

Abstract

This study investigated osteogenesis of human mesenchymal stem cells (hMSCs) encapsulated in matrix-metalloproteinase (MMP)-sensitive poly(ethylene glycol) (PEG) hydrogels in chemically-defined medium (10 ng/ml BMP-2). Thiol-norbornene photoclick hydrogels were formed with CRGDS and crosslinkers of PEG dithiol (non-degradable), CVPLS-LYSGC (P1) or CRGRIGF-LRTDC (P2) (dash indicates cleavage site) at two crosslink densities. Exogenous MMP-2 degraded P1 and P2 hydrogels similarly. MMP-14 degraded P1 hydrogels more rapidly than P2 hydrogels. Cell spreading was greatest in P1 low crosslinked hydrogels and to a lesser degree in P2 low crosslinked hydrogels, but not evident in non-degradable and high crosslinked MMP-sensitive hydrogels. Early osteogenesis (ALP activity) was accelerated in hydrogels that facilitated cell spreading. Contrarily, late osteogenesis (mineralization) was independent of cell spreading. Mineralized matrix was present in P1 hydrogels, but only present in P2 high crosslinked hydrogels and not yet present in non-degradable hydrogels. Overall, the low crosslinked P1 hydrogels exhibited accelerated early and late osteogenesis with the highest ALP activity (day 7), greatest calcium content (day 14), and greatest collagen content (day 28), concomitant with increased compressive modulus over time. Collectively, this study demonstrates that in chemically-defined medium, hydrogel degradability is critical to accelerating early osteogenesis, but other factors are important in late osteogenesis.

Keywords

Matrix-metalloproteinase; hydrogel; mesenchymal stem cell; osteogenesis; extracellular matrix

[*]corresponding Author Stephanie Bryant, 3415 Colorado Ave, Boulder, CO 80309-0596, Phone: 303-735-6714, stephanie.bryant@colorado.edu.

The authors have no conflict of interest.

Introduction

In situ delivery of stem cells within an injectable and degradable hydrogel is a promising minimally invasive approach for the reconstruction of damaged bone (Gibbs et al., 2016). Synthetic-based hydrogels offer a high degree a tunability where adhesion peptides and crosslinks that are sensitive to cell-secreted matrix metalloproteinases (MMPs) can be introduced with high fidelity, creating environments that mimic the native extracellular matrix (ECM) microenvironment (Tibbitt and Anseth, 2009). Altering the crosslink density and/or the chemistry of the crosslinker, for example, enables control over the rate of hydrogel degradation (Nicodemus and Bryant, 2008). Moreover, degradation of the hydrogel is critical to cell spreading and necessary for deposition of cell-secreted extracellular matrix (ECM) (Marie, 2013). Thus, hydrogel degradability is an important design parameter for MSC differentiation and tissue engineering.

Two MMP's that are critical to bone formation *in vivo* are MMP-2 and MMP-14 (Holmbeck et al., 1999; Mosig et al., 2007). MMP-2, a soluble MMP with collagenolytic activity, has the ability to cleave the main collagen, collagen type I, found in bone. MMP-14 on the other hand is a cell surface MMP, which has been shown to cleave a range of cell surface molecules to enable cell migration (Itoh, 2006). For example, MMP-14 has been shown to be involved in migration and invasion of mesenchymal stem cells (MSCs) into bone (Karsdal et al., 2004; Ries et al., 2007). The function of MMP-2 is linked to MMP-14. The latter is required to convert the pro-form of MMP-2 to its active form (Silva Paiva and Granjeiro, 2014). Both MMP-2 and MMP-14 represent potential targets to include in the design of MMP-sensitive hydrogels for bone tissue engineering.

Several studies have investigated synthetic-based hydrogels designed with MMP sensitive crosslinks for bone regeneration. For example, an acellular MMP-sensitive hydrogel, whose peptide crosslink chemistry was cleavable by MMP-2 (Patterson and Hubbell, 2010), facilitated cell infiltration and bone regeneration *in vivo* when combined with other bioactive factors (Lutolf et al., 2003). Using the same peptide crosslinker, others have encapsulated human MSCs in an MMP-sensitive hyaluronic acid hydrogel and shown that cell spreading and osteogenic differentiation were enhanced *in vitro* when compared to a MMP-insensitive peptide crosslinker (Kim et al., 2010). These and other studies demonstrate the importance of hydrogel degradability on osteogenesis.

Chemically-defined medium that is absent of serum has gained increasing interest for the *in vitro* culture of stem cells. This shift is in part due to the high degree of lot variability in fetal bovine serum (FBS) (Price and Gregory, 1982), which is commonly used in osteogenic medium. As a result, lot screening is necessary for osteogenesis *in vitro* (Haynesworth et al., 1992). Moreover, there are several growing concerns such as the immunogenicity of culturing human cells in the presence of bovine proteins (Sakamoto et al., 2007) and the decreasing availability of FBS given the increasing demand worldwide. Beyond these practical and translational issues, the presence of serum can have confounding effects on studying cellular responses *in vitro*. Relevant to MMP-sensitive hydrogels, serum contains several protease inhibitors (Ikari et al., 2000) that can inhibit MMP activity (Vincenti et al., 1996). Thus, the presence of serum has the potential to alter degradation behavior of MMP-

sensitive hydrogels making it difficult to evaluate degradation events that are specific to cell-mediated processes.

The overall goal of this study was to investigate the role of cell-mediated hydrogel degradability, as a result of differences in the crosslink density and chemistry of the crosslinker, on the osteogenic capacity of encapsulated human MSCs (hMSCs) in chemically-defined medium. The latter was chosen to avoid confounding results by the presence of serum. A cytocompatible PEG hydrogel based on the thiol-norbornene photoclick chemistry was chosen for its ease with which to incorporate cysteine containing peptides (Fairbanks et al., 2009a) and for its promise in bone tissue engineering (Anderson et al., 2011; Fairbanks et al., 2009b; Khetan et al., 2013b). Two peptide crosslinkers were chosen for this study based on the MMP-sensitive sequences of VPLS-LYSG and GRIGF-LRT, where the dash indicates the cleavage site. These two peptides were selected based on their reported substrate reactivity to MMP-2 (Amer and Bryant, 2016; Turk et al., 2001) and MMP-14 (Kridel et al., 2002), respectively. A schematic of the hydrogel and its formation are shown in Figure 1. The cell adhesion peptide RGD was included to facilitate cell attachment and support cell spreading during degradation. The hydrogels were cultured in chemically-defined medium supplemented with bone morphogenic factor-2 (BMP-2) at a low concentration of 10 ng/ml. This BMP-2 concentration was chosen because it has been shown to be insufficient at early times, but effective at longer culture times, to induce osteogenesis, while ≥50 ng/ml rapidly induce osteogenesis (Gori et al., 1999; Knippenberg et al., 2006; Lecanda et al., 1997). Thus, using a low concentration of BMP-2 will prevent saturation of BMP signaling and enable the effects of hydrogel properties on osteogenic capacity to be assessed.

The specific aims of this study were three-fold. First, degradation of acellular hydrogels crosslinked with these two peptides by exogenous MMP-2 and MMP-14 were investigated. Second, the effect of degradability on cell shape of encapsulated hMSCs in the hydrogel was assessed. Third, the osteogenic capacity of hMSCs encapsulated in the MMP-sensitive hydrogels was assessed. The latter two were determined as a function of two crosslink densities for the two peptide crosslinkers. Osteogenic capacity was evaluated by alkaline phosphatase activity, collagen deposition, and mineral and compared to a nondegradable PEG hydrogel as a control.

Materials and Methods

Monomer Synthesis

Multi-arm PEG functionalized with norbornene was synthesized by reacting an 8-arm PEG-NH_2 of molecular weight 20,000 g/mol (JenKem Technology USA, Plano, TX) with 5-norbornene-2-carboxylic acid (Sigma-Aldrich, St. Louis, MO) using the coupling reagents, 2-(1H-7-azabenzotriazol-1-yl)-1,1,3,3-tetramethyl uranium hexafluorophosphate methanaminium (HATU) (Chem-Impex International, Inc., Wool Dale, IL), and N,N-diisopropylethylamine (DIPEA) (Chem-Impex). The reaction was carried out in dimethylformamide (DMF) and dichloromethane (DCM) (Sigma-Aldrich) at room temperature under argon and overnight. The final product was recovered by precipitation in diethyl ether (Sigma-Aldrich) and purified by dialysis in water. ^{1}H NMR was used to

confirm >90% of the arms were functionalized with norbornene. Peptide crosslinkers CVPLS-LYSGC and CRGRIGF-LRTDC were purchased (GenScript).

Fabrication of Hydrogels

MMP-sensitive hydrogels were formed from a solution containing 3 or 6% (g/g) 8-arm PEG norbornene monomer, peptide crosslinker at a 0.8:1 thiol:ene ratio, 2 mM CRGDS (GenScript), with 0.05% (g/g) photoinitiator, 1-(4-(2- Hydroxyethoxy)-phenyl)-2-hydroxy-2-methyl-1-propane-1-one (I2959; BASF, Tarrytown, NY) in phosphate-buffered saline (PBS). Nondegradable hydrogels were formed from a solution containing 3 or 6% (g/g) of 8-arm PEG-norbornene monomer, PEG-dithiol crosslinker (1000 g/mol; Sigma-Aldrich) at 0.6:1 thiol:ene ratio, 2 mM CRGDS, and 0.05% (g/g) I2959. Solutions were polymerized under 352 nm light at 5–10 mW/cm^2 for 10 min. Hydrogel formulations are given in Table 1 for hydrogels referred to herein as soft and stiff hydrogels.

Acellular Hydrogel Degradation by Exogenous Enzymes

Cylindrical acellular hydrogels (3 mm diameter and 3 mm height) of the low crosslinked hydrogel formulation were fabricated as described above, but without CRGDS and in Milli-Q water. Hydrogels were placed in a buffer solution appropriate for each enzyme and allowed to swell to equilibrium for 48 hours. MMP-2 enzyme buffer was 50 mM HEPES, 10 mM $CaCl_2$, 20% glycerol, and 0.005% BRIJ-35. MMP-14 enzyme buffer was 150 mM NaCl, 50 mM Tris-HCl, 5 mM $CaCl_2$. After equilibrium swelling, the buffer solution was replaced with their respective buffers containing either 0.5 nM MMP-2 (Calbiochem, EMD Millipore) or 1.5 nM MMP-14 (Calbiochem, EMD Millipore) and incubated at 37°C. Samples were collected daily for 7 days, with enzyme solutions refreshed every 24 hours.

Characterization of Acellular Hydrogel Degradation

Acellular swollen hydrogels (n=3) were collected at prescribed times (described above). Hydrated samples were weighed (wet weight, mw). The compressive modulus was measured using a Mechanical Testing System (MTS with 10 N load cell; Eden Prairie, MN). Samples were tested in unconfined compression with a 2 mN pre-load and the subjected to a strain rate of 0.5 mm/min applied to 15% strain. The slope of the stress–strain curve between 10 and 15% strain was used to determine the compressive modulus. Samples were subsequently lyophilized and dry weights measured (dw). The mass swelling ratio (q) was determined from mw/dw.

Cell Culture and Encapsulation

Primary human MSCs (hMSCs) were obtained from Texas A&M University Health Science Center and College of Medicine, Institute for Regenerative Medicine. MSCs were plated at 3000 $cells/cm^2$ and expanded in growth media consisting of Modified Essential Medium (MEM) α (Gibco) supplemented with 10% FBS (Atlanta Biologicals), 5 ng/mL recombinant human FGF-basic (Peprotech), and penicillin/streptomycin/amphotericin B (PSF, Invitrogen) and under standard cell culture conditions (at 37°C with 5% CO_2). Medium was exchanged three times weekly and cells were expanded ~80–90% confluency per passage until passage 4.

hMSCs were encapsulated into the MMP-sensitive and nondegradable hydrogels at 10×10^6 cells/mL of hydrogel precursor solution. For the cellular hydrogels, 2 mM CRGDS was added to the precursor solution prior to polymerization. Cell-laden hydrogels were cultured in defined osteogenic differentiation media consisting of Modified Essential Medium (MEM) α (Gibco) supplemented with 10 ng/mL bone morphogenetic protein-2 (BMP-2; Peprotech), 1x ITS+ premix (Corning), 100nM dexamethasone (Sigma-Aldrich), 50 μg/mL acorbate-2-phosphate (Sigma-Aldrich), 1x MEM non-essential amino acids (Gibco), 10 mM β-glycerophosphate (Sigma-Aldrich) and penicillin/streptomycin/amphotericin B (PSF, Invitrogen). Cell-laden hydrogels were cultured under standard cell culture conditions. A separate set of acellular hydrogels was also cultured.

Cell Viability and Shape

Cell viability (n=2) was qualitatively assessed on day 1 and 28 by live/dead assay based on Calcein AM, which stains the cytosol of live cells, and ethidium homodimer, which enters the nucleus of compromised cells and stains DNA. Hydrogel constructs were incubated in osteogenic media with 4 μM Calcein AM for 10 minutes, after which ethidium homodimer was incorporated at 2 μM and hydrogels were incubated for another 10 minutes. Hydrogels were immediately imaged using confocal microscopy (Zeiss LSM 5 Pascal system using a Zeiss Axiovert microscope) with either a 10x or 40x objective. Cell shape (n=2) was quantified from the live/dead confocal microscopy images using NIH Image J and the particle analyzer measurement for circularity. A minimum threshold was set for area to remove cells that were out of plane in the image. Aggregates of cells were not counted.

Biochemical Assays

Hydrogel constructs (n=3) were removed from culture at days 7, 14, and 28, rinsed in PBS for 1 hr, lysed in deionized water (diH_2O), snap frozen in liquid nitrogen and stored at −80°C. Samples were disrupted using a tissue lyser (Qiagen), then prepared through freeze-thaw-sonicate cycles to lyse the cells. A known amount of the sample was removed for each subsequent assay. DNA content was measured using a Quant-iT PicoGreen dsDNA Assay Kit (Thermo Fisher Scientific) with fluorescence at 480 nm excitation and 520 nm emission according to manufacturer specifications. A stock lambda DNA standard provided in the kit was used. Alkaline phosphatase activity was determined as the number of moles of p-nitrophenol phosphate catalyzed to p-nitrophenol by measuring absorbance at 405 nm using a spectrophotometer, with p-nitrophenol (Sigma) as the standard. Total calcium was measured using the Calcium (CPC) Liquicolor® Assay (Stanbio) according to manufacturer specifications, with absorbance measured at 540 nm. A stock calcium standard provided in the kit was used. Calcium content was also measured in the acellular hydrogels, which arises due to the culture medium. The calcium content in the acellular hydrogels was subtracted from the cellular hydrogels. For total collagen content, samples were digested in 1 mg/ml pepsin (Worthington) in 0.5 M acetic acid overnight prior to being incubated with 5 mg/ml Sirius Red (Sigma) for 30 min. Rat-tail type I collagen (BD Biosciences) was used as the standard. Absorbance was measured at 540 nm using a spectrophotometer.

Histological Analysis

Hydrogel constructs (n=3) were removed from culture at day 28 and immediately fixed in 4% paraformaldehyde at 4°C for 24 hr. Samples were subjected to dehydration and paraffin embedding following standard protocols. Sections of 10 μm in thickness were prepared. For collagen type I staining, sections were first pretreated with pepsin (280 kU), protease (400 U) and 0.25%trypsin and EDTA for 1 h at 37C followed by antigen retrieval. Following, the sections were blocked with 1% BSA, washed twice, and permeabilized with 1% BSA 0.25% Triton-X-100. Sections were treated with primary anti-collagen type I (1:50, Abcam ab34710) followed by secondary antibodies with conjugated AlexaFluor 546 probes and counterstained with DAPI for nucleus detection. Stained sections were imaged using confocal microscopy (Zeiss LSM 5 Pascal). A separate set of sections were stained following the von Kossa protocol with nuclear red counter stain. Tissue sections were imaged using light microscopy (Zeiss Axiovert microscope).

Statistics

Data are presented as the mean with standard deviation reported parenthetically in the text and as error bars in the figures. Statistical analysis was performed using Real Statistics add-in for Excel. For the acellular hydrogel degradation experiments, an unpaired t-test was performed to compare the equilibrium compressive modulus and mass swelling ratio for the two enzyme swelling solvents. A two-way balanced ANOVA (α=0.05) was performed with peptide crosslinker and time as factors for acellular hydrogel degradation. The cellular experiments (circularity, DNA/construct, ALP/DNA, total collagen content, total calcium) were analyzed by a three-way fixed ANOVA (α=0.05). Factors were hydrogel type (P1, P2, non-degradable), crosslinking (low and high), and culture time. If the three-way interaction was statistically significant or all three two-way interacts were statistically significant, follow-up two-way ANOVAs were performed. In that case, the two-way ANOVA results are presented. Post-hoc analysis was performed by Tukey's HSD with α=0.05. A *p*-value of <0.05 was considered statistically significant.

Results

Degradation of hydrogels by exogenous enzymes

MMP-sensitive hydrogels were prepared with the peptide crosslinkers CVPLS-LYSGC or CRGRIGF-LRTDC to form P1 and P2 hydrogels, respectively (Figure 1). Low crosslinked hydrogels were used to evaluate susceptibility of the hydrogels to MMP-2 and MMP-14 enzymes. The mass swelling ratio and compressive modulus were measured at equilibrium prior to degradation and as a function of time in the presence of exogenous MMP-2 or MMP-14 in the solvent appropriate for each enzyme (Figure 2). Differences in the equilibrium properties (prior to introducing the enzyme) in the MMP-2 buffer solution were observed due to crosslinker chemistry as shown in Figure 2A,B. Exogenous degradation of the P1 and P2 hydrogels by MMP-2 followed similar degradation patterns. The mass swelling ratio (*q*) increased (p<0.001) with time for both hydrogels (Figure 2C). Hydrogel type was a factor affecting (p<0.001) the mass swelling ratio, but pairwise comparisons revealed a difference only at day 7 where q was higher (p=0.001) for P1 hydrogels. The

normalized modulus decreased (p<0.001) with time with no significant differences between the hydrogels (Figure 2D).

For the MMP-14 experiments, differences in equilibrium properties (prior to introducing the enzyme) in the MMP-14 buffer solution were observed due to crosslinker chemistry as shown in Figure 2E,F. When exposed to MMP-14 enzyme, the mass swelling ratio increased (p<0.001) with time for both hydrogels, but there was no significant difference between the hydrogels prior to them reaching reverse gelation (Figure 2G). The normalized modulus for both the P1 and P2 hydrogels decreased (p<0.001) with time when exposed to MMP-14, eventually reaching reverse gelation within the time frame of the experiment (Figure 2H). The modulus was lower (p<0.001) for the P1 hydrogels when compared to the P2 hydrogels, indicating faster degradation.

Collectively, the swelling ratio and modulus results indicate the P1 hydrogels are more susceptible to the enzyme MMP-14 than are P2 hydrogels. On the contrary, the degradation behavior for both P1 and P2 hydrogels is similar in response to MMP-2.

MSC viability and shape in the hydrogels

Human MSCs were encapsulated in each hydrogel type (non-degradable, P1 and P2) and hydrogel crosslink density (low and high) and assessed for viability and cell shape (Figure 3). Day 1 represents the viability and cell shape as a result of encapsulation in the hydrogels. Day 28 represents the long-term effects of the 3D culture environment on viability and on cell shape as a result of cell-mediated degradation. Encapsulated cells remained largely viable throughout the study with some visible staining for dead cells at day 1 and 28 (Figure 3A).

Cell shape was quantified by measuring circularity of live cells from the confocal microscopy images at days 1 and 28 (Figure 3B). A value of one indicates a perfectly circular cell while a value less than one indicates deviation from a perfect circle. A three-way ANOVA revealed a significant three-way interaction (p=0.003). Follow-up two-way ANOVAs were performed with pairwise comparisons reported (Figure 3C). For the non-degradable hydrogels, the cells remained rounded with a circularity of ~0.9 for both crosslinked hydrogels and at both time points. For the MMP-sensitive hydrogels at both crosslink densities, the cells remained rounded with a circularity of ~0.8 at day 1. The low crosslinked P1 hydrogels exhibited a decrease (p=0.004) in circularity from day 1 to day 28 to a value of 0.32. The low crosslinked P2 hydrogels also exhibited a decrease (p=0.005) in circularity from day 1 to day 28 to a value of 0.65. At day 28, the circularity was lower (p=0.04) for P1 hydrogels compared to the P2 hydrogels. For the high crosslinked MMP-sensitive hydrogels, there was no significant change in the circularity regardless of peptide at day 28 and the cells remained rounded.

Collectively, these results demonstrate that encapsulated hMSCs remained viable throughout the experiment. Cell spreading was evident in the P1 hydrogels and to a lesser degree in the P2 hydrogels for the low crosslinked experimental group, but minimal cell spreading was observed in the high crosslinked MMP-sensitive hydrogels and in the non-degradable hydrogels regardless of crosslinking.

Cell number and alkaline phosphatase activity in the hydrogels

The total number of cells within the hydrogel constructs was assessed by measuring double stranded DNA content in each hydrogel type (non-degradable, P1 and P2) and hydrogel crosslink density (low and high) over culture time (Figure 4A). A three-way ANOVA did not identify a significant three-way interaction between the factors, but did reveal significant interactions between all two-way interactions. Select follow-up two-way ANOVAs were performed (Figure 4B) followed by pairwise comparisons. DNA content in the non-degradable hydrogels remained constant over time in the low crosslinked hydrogels, but decreased in the high crosslinked hydrogels (e.g., 76% from day 7 to day 28, $p<0.001$). In P1 hydrogels, DNA content increased for the low crosslinked hydrogels (e.g., 60% from day 7 to day 28, $p=0.005$), but did not change with time for the high crosslinked hydrogels. For the P2 hydrogels, DNA content remained constant for the low crosslinked hydrogels, but decreased for the high crosslinked hydrogels (e.g., 70% from day 7 to day 28, $p<0.001$) with time. Overall, the P1 hydrogels maintained the highest DNA content with low crosslinked hydrogels having the highest DNA content at day 28.

Early osteogenesis of encapsulated hMSCs was determined by alkaline phosphatase (ALP) activity normalized to DNA content in each hydrogel type (non-degradable, P1 and P2) and hydrogel crosslink density (low and high) over culture time (Figure 4C,D). A three-way ANOVA with culture time, hydrogel type, and crosslink density revealed a significant ($p=0.006$) three-way interaction between the factors. Select follow-up two-way ANOVAs were performed (Figure 4E) with pairwise comparisons reported.

In the low crosslinked hydrogels, ALP activity was highest ($p\leq0.002$) in the P1 hydrogels at day 7 and highest ($p\leq0.001$) in the P2 hydrogels at day 14. By day 28, the non-degradable and P2 hydrogels had higher ($p\leq0.02$) ALP activity than the P1 hydrogels. In the high crosslinked hydrogels, ALP activity was low and similar across the three hydrogel formulations at day 7 and day 14. At day 28, ALP activity in the non-degradable and P2 hydrogels was higher ($p\leq0.03$) than the P1 hydrogels. As a function of time in non-degradable hydrogels, ALP activity was highest ($p<0.05$) at day 28, with no difference as a function of hydrogel crosslink density. In the P1 hydrogels, ALP activity was the highest ($p<0.001$) at day 7 in the low crosslinked hydrogels and then declined with time. With the high crosslinked P1 hydrogels, ALP activity was highest ($p<0.001$) at day 14 and then declined at day 28. In the P2 hydrogels, ALP activity increased ($p=0.007$) at day 14 and remained high at day 28 in the low crosslinked hydrogels. In the high crosslinked P2 hydrogels, ALP activity was highest ($p=0.005$) at day 28.

Collectivity, these results indicate that ALP activity was highest initially in the low crosslinked P1 hydrogels among the other hydrogel formulations and decreased over time. The low crosslinked P2 hydrogels increased by day 14 and remained high while the remaining other hydrogel formulations showed elevated ALP activity the latest at day 28.

Total collagen content in the hydrogels

Total collagen content was assessed in each hydrogel type (non-degradable, P1 and P2) and hydrogel crosslink density (low and high) over culture time (Figure 5). A three-way ANOVA

revealed a significant (p<0.0001) three-way interaction for total collagen content per construct. Follow-up two-way ANOVAs were performed (Figure 5B) with pairwise comparisons reported. In non-degradable hydrogels, there was minimal collagen content in the low crosslinked hydrogel with no significant change with culture time. In the high crosslinked hydrogels, collagen content increased (p=0.008) by day 14, but then decreased (p=0.02) at day 28 to levels that were not different from the initial time point. In the P1 hydrogels, collagen content increased by 2.7-fold (p<0.001) and 1.3-fold (p=0.03) from day 7 to 28 in the low and high crosslinked hydrogels, respectively. In the P2 hydrogels, collagen content increased by 2.6-fold from day 7 to 28 in the low crosslinked hydrogels. In the high crosslinked P2 hydrogels, collagen content increased (p<0.001) by 1.8-fold from day 7 to 14, but then decreased (p=0.005) at day 28 to levels that were not different from day 7. Across the low crosslinked hydrogels, total collagen content was highest (p<0.001) in the P1 hydrogel with the P2 hydrogel having higher (p<0.001) contents over the non-degradable hydrogels. Across the high crosslinked hydrogels, P1 hydrogels were higher (p=0.009) than the non-degradable hydrogels at day 28, while the P2 hydrogels were higher (p=0.03) than the non-degradable hydrogels at day 14. There was no difference between P1 and P2 hydrogels. Overall, these results demonstrate that total collagen content deposited into the hydrogels was the highest in the low crosslinked P1 hydrogels. It should be noted that this high collagen content correlates with the hydrogel that had the highest DNA content at the end of the study.

The spatial localization of collagen type I was also assessed and representative images at two magnifications are shown in Figure 5C. Collagen type I was present and localized to the pericellular regions in all experimental groups at day 28. The non-degradable hydrogels appeared to have the least amount of pericellular staining regardless of hydrogel crosslinking. In the degradable P1 and P2 hydrogels, there was evidence of collagen interconnectivity between cells and some regions that were more expansive than others. However, there were no obvious differences in the spatial deposition of collagen type I among the MMP-sensitive hydrogels.

Mineralization in the hydrogels

Mineralization was assessed quantitatively by total calcium content for each hydrogel type (non-degradable, P1 and P2) and hydrogel crosslink density (low and high) over culture time (Figure 6). A three-way ANOVA revealed a significant (p=0.004) three-way interaction for total calcium content per construct (Figure 6A). Follow-up two-way ANOVAs were performed (Figure 6B) with pairwise comparisons reported. In all hydrogels, there was no detectable calcium at day 7 over the acellular controls. In the non-degradable hydrogels, there was no detectable calcium in the hydrogels at day 14 with some calcium being detected by day 28. In the low crosslinked P1 hydrogels, calcium was present by day 14, which increased further (p=0.02) by day 28. Calcium content was lower (p=0.01) with higher crosslinking at day 14 but by day 28 the content was similar in the low and high crosslinked P1 hydrogels. In the P2 hydrogels, calcium content was detected in the low crosslinked by day 14 and 28, but the levels were low. Calcium content was higher (p<0.001) in the high crosslinked hydrogels at day 28. Across the low crosslinked hydrogels, total calcium content was highest (p<0.001) in the P1 hydrogel by day 28. Across the high

crosslinked hydrogels, calcium content was highest ($p<0.01$) in the P1 hydrogels by day 28, followed by the P2 hydrogels, which were higher ($p<0.001$) than the non-degradable hydrogels. Overall, these results demonstrate that total calcium content deposited into the hydrogels was the highest in the P1 hydrogels, but was not affected by crosslinking.

Von Kossa staining indicated mineral deposits localized to the pericellular regions at day 28 (Figure 6C). The presence of mineral deposits mirrored that of the total calcium per construct with P1 hydrogels showing the greatest positive staining in the low and high crosslinked hydrogels. In the high crosslinked P2 hydrogels, there was evidence of pericellular localization of mineral deposits. There was minimal staining in the low crosslinked P2 hydrogels and in the non-degradable hydrogels.

Mechanical properties of the cell-laden hydrogels

Compressive modulus was assessed for each hydrogel type (non-degradable, P1 and P2) and hydrogel crosslink density (low and high) over culture time (Figure 7A). A three-way ANOVA did not identify a significant three-way interaction between the factors, but did reveal significant interactions between all two-way interactions. Follow-up two-way ANOVAs were performed (Figure 7B) with pairwise comparisons reported. For the non-degradable hydrogels, there was no significant change in modulus with culture time, but the high crosslinked hydrogels retained ($p<0.001$) a higher modulus during the experiment. Similar findings were reported for the P2 hydrogels. On the contrary, the compressive modulus for the P1 hydrogels was affected by time ($p=0.02$) and hydrogel crosslinking ($p<0.001$). The modulus of the high crosslinked P1 hydrogels remained higher ($p<0.001$) than the low crosslinked hydrogels at all time points. For the low crosslinked hydrogels, the modulus at day 28 was higher ($p<0.05$) when compared to all of the time points. For the high crosslinked hydrogels, the modulus decreased with time where day 1 was higher ($p<0.05$) than all other time points, but days 7, 14, and 28 were not significantly different from each other. These data indicate that P1 hydrogels experienced the greatest changes in modulus with the low crosslinked hydrogels exhibiting an increase in modulus over time and the high crosslinked hydrogels exhibiting a decrease in modulus over time.

Discussion

This study demonstrated osteogenic capacity of hMSCs when encapsulated in MMP-sensitive hydrogels and cultured in chemically-defined osteogenic medium, but in a manner that depended on the hydrogel environment. Hydrogel degradability was required for cells to spread and of the two MMP's investigated, hydrogels that were more sensitive to MMP-14 compared to MMP-2 led to a greater degree of spreading. The temporal response of early osteogenesis correlated with the degree of cell spreading. On the contrary, cell spreading and early osteogenesis did not correlate with the ability of the encapsulated cells to synthesize a mineralized matrix. These findings suggest that cell spreading may accelerate early osteogenesis, but may not be required for late stage osteogenesis.

This study utilized chemically-defined media with a low concentration BMP-2 to support osteogenesis, but minimize confounding factors associated with serum. Our results demonstrate that under certain conditions, mineral deposits, which is a characteristic feature

defining osteogenesis, are present. This observation confirms that osteogenesis was supported under the chemically-defined medium. However, our results also suggest a delay in osteogenesis. Notably, in the non-degradable hydrogels a late increase in ALP activity was observed, but with minimal evidence of mineral deposits at day 28. Other studies have reported mineral deposition by hMSCs encapsulated in non-degradable PEG hydrogels when cultured under normal osteogenic medium containing fetal bovine serum (Nuttelman et al., 2004; Steinmetz and Bryant, 2011). Differences in osteogenic capacity reported herein can therefore be attributed to the hydrogel environment.

The MMP-sensitive hydrogels investigated in this study were formed from peptide crosslinks based on sequences known to be cleaved by MMP-2 and/or MMP-14. Herein, we show that both peptide sequences are susceptible to MMP-2 and MMP-14. The P1 sequence has been previously tested in solution for its susceptibility to MMP-2 and MMP-14 (Turk et al., 2001), which is consistent with our findings. The P2 sequence was identified based on its greater specificity to MMP-14 over MMP-2 (Kridel et al., 2002), but we demonstrate its susceptibility to both MMP-2 and MMP-14. Specifically, exogenous degradation studies revealed that P1 and P2 hydrogels were similarly susceptible to MMP-2, but P1 hydrogels were more susceptible to MMP-14 than the P2 hydrogels. However, it is important to note that many peptide sequences are susceptible to multiple MMPs, albeit with different kinetics. For example, the P1 sequence in solution has been reported to be susceptible to MMP 1–3, 7 and 9 with the highest k_{cat}/K_m towards MMP-2 (Patterson and Hubbell, 2010). The P2 sequence was described to have a 40-fold higher k_{cat}/K_m towards MMP-14 compared to MMP-9 in solution (Kridel et al., 2002). MSCs, on the other hand, have been shown to express MMP 1, 2, 13, 14, and 16 with MMP-14 being the only one of these five collagenolytic MMPs that was essential to mediating cell shape and supporting osteogenic differentiation in 3D collagen gels (Lu et al., 2010). Although this study did not identify the specific cell-derived MMP involved in hydrogel degradation, the P1 hydrogel which exhibited faster degradation by exogenous MMP-14 correlated to a greater change in cell shape. The latter indicates there was more cell-mediated hydrogel degradation. We surmise that MMP-14 is the likely MMP that is involved in differentially mediating hydrogel degradation prepared from these two peptides. However, additional studies are needed to confirm the specific MMP(s) involved.

MMP-14 is present on the cell membrane, which will lead to cleavage of the hydrogel crosslinks within the pericellular environment while not affecting the bulk hydrogel. Contrarily, MMP-2 is a soluble MMP whose size is small enough to diffuse through the hydrogels, leading to bulk hydrogel degradation. This observation is supported by estimates of hydrogel mesh size, which can be determined from the hydrogel properties of volumetric swelling, compressive modulus, and crosslink density (Bryant and Anseth, 2005). The initial mesh size (i.e., prior to degradation) is estimated at ~20 nm for the stiff hydrogel and ~60 nm for soft hydrogels, which is larger than the size of most soluble MMPs, including MMP-2 at ~7–10 nm (Morgunova et al., 1999; Ross et al., 2012). A decrease in modulus, albeit slight but significant, was observed for the MMP-sensitive hydrogels (with the exception of the low crosslinked P1 hydrogel). This result suggests that bulk degradation occurred due to diffusing MMPs. However, it does not appear to be the predominant degradation mechanism, given that substantial cell spreading was observed. With higher

crosslinking, the encapsulated cells retained their round morphology indicating that there were too many crosslinks and/or insufficient matrix degrading enzymes to degrade the bulk hydrogel. This observation further supports the role of MMP-14, but again additional experiments are needed to confirm the exact MMPs involved.

The osteogenic capacity of encapsulated hMSCs was improved in low crosslinked P1 hydrogels. Early osteogenesis was evaluated by ALP activity, which peaks during differentiation and then subsides (Huang et al., 2007). Late osteogenesis was evaluated by mineralization. In this hydrogel, ALP activity was the highest at day 7 when compared to the other hydrogel formulations and then declined at day 14, suggesting that ALP had peaked prior to day 14. The other hydrogel formulations showed an apparent peak in ALP activity at later times (i.e., around day 14 or 28), but with a magnitude that was greater than the P1 hydrogels. We attribute differences in magnitude to the timing of when ALP activity was measured. Late osteogenesis was also evident in this hydrogel formulation, where an increase in calcium content was observed by day 14 and was higher than the other hydrogel formulations. Moreover, by day 28 accumulated ECM of collagen and calcium contents was the greatest in this hydrogel, which contributed to the increase in construct stiffness over time. Overall, the low crosslinked P1 hydrogel supported early and late osteogenesis of the encapsulated hMSCs when cultured in chemically-defined culture medium.

The other hydrogel formulations displayed temporal differences in early and late osteogenesis. For example, the low crosslinked P2 hydrogels, which supported cell spreading, had the highest ALP activity at day 14, but did not support mineralization by day 28. High crosslinked P1 and P2 hydrogels did not promote significant cell spreading, but supported late osteogenesis. The non-degradable hydrogels showed signs of early osteogenesis by day 28 with elevated ALP activity, but did not support late osteogenesis by day 28. These disparate findings suggest that cell spreading may accelerate early osteogenesis, but other mechanisms within the MMP-sensitive hydrogels may be driving late osteogenesis associated with mineralized ECM deposition.

A number of studies have linked cell shape to early osteogenesis as measured by ALP activity (Mathieu and Loboa, 2012). For example, Wang *et al.*(Wang et al., 2012) reported that controlling cell shape on micropatterned substrates led to increases in cytoskeletal tension and augmented BMP-2 induced osteogenesis. Other studies, however, have indicated that it is adhesion strength and not cell shape that drives osteogenesis (Khetan et al., 2013a; Wang et al., 2016). Furthermore, cytoskeleton tension has been shown to be higher when cells are encapsulated in degradable hydrogels compared to non-degrading hydrogels, despite having the same amount of adhesion peptides (Khetan et al., 2013a). Herein, cell adhesion is initially mediated by RGD peptides tethered into the hydrogel, which was similar across all hydrogels. We therefore postulate that early differentiation, as measured by ALP activity, is augmented by the ability of the cells to degrade, spread and develop higher cytoskeleton tension leading to earlier induction in BMP2-induced osteogenesis, which was observed in the low crosslinked P1 hydrogels followed by the P2 hydrogels.

Interestingly, late stage osteogenesis as measured by a mineralized matrix did not correlate to the degree of cell spreading or the observed early induction of osteogenesis by ALP

activity. Mineralization was localized to the pericellular matrix and spatially correlated with collagen deposition. Collagen type I can serve as a nucleation site for mineralization (Chen et al., 2015), but only when other non-collagenous cell-secreted proteins (e.g., osteocalcin) (Nakamura et al., 2009) are present. There are several possible factors contributing to the observed results. Mineralization was supported in the high crosslinked MMP-sensitive hydrogels, regardless of peptide chemistry, but was not supported in the high crosslinked non-degradable hydrogels despite having similar matrix stiffness. Although cell spreading was not detectable in any of these hydrogels, we cannot rule out the possibility that the MMP-sensitive hydrogels facilitated the formation of dendritic-like cellular processes, which is a characteristic feature of late osteogenesis and for which MMP-14 is known to be involved (Bonewald, 2011). These processes are much smaller than those associated with cell spreading, reported to have diameters of ~0.1–0.2 μm (You et al., 2004). Therefore, they may be difficult to visualize in our confocal microscopy images. Although the diameter of dendrites is small, they are still larger than the mesh size of the hydrogel, thus requiring degradation. It was surprising that the low crosslinked P2 hydrogels did not support mineralization. It is possible that matrix stiffness and subsequently cytoskeletal tension is still playing a role. Several studies have shown a correlation with increasing matrix stiffness and higher expression of late osteogenic markers, such as osteocalcin (Shih et al., 2011; Zhang et al., 2017). The low crosslinked P2 hydrogels exhibited a decrease in stiffness with time and resulted in the lowest stiffness at day 28 compared to the other MMP-sensitive hydrogels, which supported mineralization. The concentration of cell-secreted soluble MMPs (e.g., MMP-2) will be highest at the cell surface and as MMPs diffuse away radially from the cell surface, their concentration will decrease such that bulk degradation of the hydrogel will be greater near the cell surface. This effect would result in a lower modulus near the cell than the bulk. Thus it is possible that adhesion strength was initially high to support early osteogenesis, but decreased below a certain threshold that prevented late stage osteogenesis. Further studies are needed to determine the exact mechanisms that mediate late stage osteogenesis in the MMP-sensitive hydrogels, but it is likely that multiple mechanisms are at play.

Collagen type I deposition was present in all hydrogel formulations and localized to regions near the encapsulated cell. Procollagen molecules are secreted by cells and assemble extracellularly to form long and mature collagen fibers. While degradation increases the hydrogel's mesh size, the assembled collagen fibers are too large to be transported through the hydrogel until reverse gelation is reached (Bryant and Vernerey, 2018). Thus, collagen deposition and accumulation will be limited to the pericellular space, which was observed in this study. It is worth noting that total collagen content was highest in the P1 low crosslinked hydrogels, but this correlated with highest number of cells. Moreover, with local degradation of the hydrogel around the cells, it is possible that collagen type I deposition will be more expansive, although less dense, due to the available space. The presence of collagen type I, but a lack of mineral deposits in some of the hydrogel formulations further suggests a delay in osteogenesis.

In conclusion, this study demonstrates that MMP-sensitive PEG hydrogels enhance osteogenesis of encapsulated hMSCs, but in a manner that depends on cell-mediated hydrogel degradability. Our results demonstrate that a hydrogel with increased susceptibility

to MMP-14 compared to MMP-2 leads to greater cell spreading and accelerates early and late osteogenesis leading to a mineralized and collagenous matrix. Our findings point to the role of cell-mediated hydrogel degradation in facilitating cell spreading and accelerating early osteogenesis. On the other hand, deposition of a mineralized ECM appears to be independent of the degree of cell spreading, suggesting that other mechanisms beyond cell shape may be important in late stage osteogenesis. These findings suggest differential temporal regulation of early and late stage osteogenesis that is dependent on the hydrogel environment. Further studies are required to identify the exact mechanisms involved. While these studies were performed in chemically-defined medium, the *in vivo* environment will contain endogenous MMPs and inhibitors of MMPs that may influence hydrogel degradation behavior. Nonetheless, this study identified that a hydrogel susceptible to MMP-14 is a promising platform to deliver MSCs for bone tissue engineering.

Acknowledgments

The authors acknowledge technical assistance from Archish Muralidharan and Leila Saleh for collagen type 1 immunohistochemistry. Research reported in this study was supported by the National Institute of Arthritis and Musculoskeletal and Skin Diseases of the National Institutes of Health under Award Number 1R01AR069060. The content is solely the responsibility of the authors and does not necessarily represent the views of the National Institutes of Health.

Grant Number: NIH 1R01AR0690604

References

Amer LD, Bryant SJ. 2016 The In Vitro and In Vivo Response to MMP-Sensitive Poly(Ethylene Glycol) Hydrogels. Annals of Biomedical Engineering 44:1–11. [PubMed: 26620776]

Anderson SB, Lin C-C, Kuntzler DV., Anseth KS. 2011 The performance of human mesenchymal stem cells encapsulated in cell-degradable polymer-peptide hydrogels. Biomaterials 32:3564–3574. [PubMed: 21334063]

Bonewald LF. 2011 The Amazing Osteocyte. Journal of Bone and Mineral Research 26:229–238. [PubMed: 21254230]

Bryant SJ, Anseth KS. 2005 Photopolymerization of hydrogel scaffolds. CRC. Scaffolding in Tissue Engineering.

Bryant SJ, Vernerey FJ. 2018 Programmable Hydrogels for Cell Encapsulation and Neo-Tissue Growth to Enable Personalized Tissue Engineering. Adv Healthc Mater 7:1–13.

Chen L, Jacquet R, Lowder E, Landis WJ. 2015 Refinement of collagen–mineral interaction: A possible role for osteocalcin in apatite crystal nucleation, growth and development. Bone 71:7–16. [PubMed: 25284158]

Fairbanks BD, Schwartz MP, Halevi AE, Nuttelman CR, Bowman CN, Anseth KS. 2009a A Versatile Synthetic Extracellular Matrix Mimic via Thiol-Norbornene Photopolymerization. Advanced Materials 21:5005–5010. [PubMed: 25377720]

Fairbanks BD, Schwartz MP, Halevi AE, Nuttelman CR, Bowman CN, Anseth KS. 2009b A Versatile Synthetic Extracellular Matrix Mimic via Thiol-Norbornene Photopolymerization. Advanced Materials 21:5005–5010. [PubMed: 25377720]

Gibbs DMR, Black CRM, Dawson JI, Oreffo ROC. 2016 A review of hydrogel use in fracture healing and bone regeneration. Journal of Tissue Engineering and Regenerative Medicine 10:187–198. [PubMed: 25491789]

Gori F, Thomas T, Hicok KC, Spelsberg TC, Riggs BL. 1999 Differentiation of human marrow stromal precursor cells: bone morphogenetic protein-2 increases OSF2/CBFA1, enhances osteoblast commitment, and inhibits late adipocyte maturation. J Bone Miner Res 14:1522–1535. [PubMed: 10469280]

Haynesworth SE, Goshima J, Goldberg VM, Caplan AI. 1992 Characterization of cells with osteogenic potential from human marrow. Bone 13:81–88. [PubMed: 1581112]

Holmbeck K, Bianco P, Caterina J, Yamada S, Kromer M, Kuznetsov SA, Mankani M, Robey PG, Poole AR, Pidoux I, Ward JM, Birkedal-Hansen H. 1999 MT1-MMP-deficient mice develop dwarfism, osteopenia, arthritis, and connective tissue disease due to inadequate collagen turnover. Cell 99:81–92. [PubMed: 10520996]

Huang Z, Nelson ER, Smith RL, Goodman SB. 2007 The sequential expression profiles of growth factors from osteroprogenitors to osteoblasts In vitro. Tissue Engineering 13:2311–2320. [PubMed: 17523879]

Ikari Y, Fujikawa K, Yee KO, Schwartz SM. 2000 α1-Proteinase Inhibitor, α1-Antichymotrypsin, or α2-Macroglobulin Is Required for Vascular Smooth Muscle Cell Spreading in Three-dimensional Fibrin Gel. Journal of Biological Chemistry 275:12799–12805. [PubMed: 10777577]

Itoh Y 2006 MT1-MMP: A key regulator of cell migration in tissue. Iubmb Life 58:589–596. [PubMed: 17050376]

Karsdal MA, Andersen TA, Bonewald L, Christiansen C. 2004 Matrix metalloproteinases (MMPs) safeguard osteoblasts from apoptosis during transdifferentiation into osteocytes: MT1-MMP maintains osteocyte viability. DNA and cell biology 23:155–65. [PubMed: 15068585]

Khetan S, Guvendiren M, Legant WR, Cohen DM, Chen CS, Burdick JA. 2013a Degradation-mediated cellular traction directs stem cell fate in covalently crosslinked three-dimensional hydrogels. Nature Materials 12:458–465. [PubMed: 23524375]

Khetan S, Guvendiren M, Legant WR, Cohen DM, Chen CS, Burdick J a. 2013b Degradation-mediated cellular traction directs stem cell fate in covalently crosslinked three-dimensional hydrogels. Nature Materials 12:458–465. [PubMed: 23524375]

Kim J, Kim IS, Cho TH, Kim HC, Yoon SJ, Choi J, Park Y, Sun K, Hwang SJ. 2010 In vivo evaluation of MMP sensitive high-molecular weight HA-based hydrogels for bone tissue engineering. J Biomed Mater Res A 95:673–681. [PubMed: 20725983]

Knippenberg M, Helder MN, Zandieh Doulabi B, Wuisman PIJM, Klein-Nulend J. 2006 Osteogenesis versus chondrogenesis by BMP-2 and BMP-7 in adipose stem cells. Biochem Biophys Res Commun 342:902–908. [PubMed: 16500625]

Kridel SJ, Sawai H, Ratnikov BI, Chen EI, Li W, Godzik A, Strongin AY, Smith JW. 2002 A unique substrate binding mode discriminates membrane type-1 matrix metalloproteinase from other matrix metalloproteinases. The Journal of biological chemistry 277:23788–93. [PubMed: 11959855]

Lecanda F, Avioli LV, Cheng SL. 1997 Regulation of bone matrix protein expression and induction of differentiation of human osteoblasts and human bone marrow stromal cells by bone morphogenetic protein-2. Journal of Cellular Biochemistry 67:386–398. [PubMed: 9361193]

Lu C, Li X-Y, Hu Y, Rowe RG, Weiss SJ. 2010 MT1-MMP controls human mesenchymal stem cell trafficking and differentiation. Blood 115:221–229. [PubMed: 19901267]

Lutolf MP, Lauer-Fields JL, Schmoekel HG, Metters AT, Weber FE, Fields GB, Hubbell JA. 2003 Synthetic matrix metalloproteinase-sensitive hydrogels for the conduction of tissue regeneration: Engineering cell-invasion characteristics. Proceedings of the National Academy of Sciences 100:5413–5418.

Marie PJ. 2013 Targeting integrins to promote bone formation and repair. Nature Reviews Endocrinology 9:288–295.

Mathieu PS, Loboa EG. 2012 Cytoskeletal and Focal Adhesion Influences on Mesenchymal Stem Cell Shape, Mechanical Properties, and Differentiation Down Osteogenic, Adipogenic, and Chondrogenic Pathways. Tissue Engineering Part B-Reviews 18:436–444. [PubMed: 22741572]

Morgunova E, Tuuttila A, Bergmann U, Isupov M, Lindqvist Y, Schneider G, Tryggvason K. 1999 Structure of human pro-matrix metalloproteinase-2: activation mechanism revealed. Science 284:1667–1670. [PubMed: 10356396]

Mosig RA, Dowling O, DiFeo A, Ramirez MCM, Parker IC, Abe E, Diouri J, Aqeel AA, Wylie JD, Oblander SA, Madri J, Bianco P, Apte SS, Zaidi M, Doty SB, Majeska RJ, Schaffler MB, Martignetti JA. 2007 Loss of MMP-2 disrupts skeletal and craniofacial development and results in

decreased bone mineralization, joint erosion and defects in osteoblast and osteoclast growth. Human Molecular Genetics 16:1113–1123. [PubMed: 17400654]

Nakamura A, Dohi Y, Akahane M, Ohgushi H, Nakajima H, Funaoka H, Takakura Y. 2009 Osteocalcin Secretion as an Early Marker of In Vitro Osteogenic Differentiation of Rat Mesenchymal Stem Cells. Tissue Engineering Part C: Methods 15:169–180. [PubMed: 19191495]

Nicodemus GD, Bryant SJ. 2008 Cell Encapsulation in Biodegradable Hydrogels for Tissue Engineering Applications. Tissue Engineering Part B 14:149–165.

Nuttelman CR, Tripodi MC, Anseth KS. 2004 In vitro osteogenic differentiation of human mesenchymal stem cells photoencapsulated in PEG hydrogels. Journal of Biomedical Materials Research Part A 68A:773–782.

Patterson J, Hubbell J a. 2010 Enhanced proteolytic degradation of molecularly engineered PEG hydrogels in response to MMP-1 and MMP-2. Biomaterials 31:7836–45. [PubMed: 20667588]

Price PJ, Gregory EA. 1982 Relationship between in vitro growth promotion and biophysical and biochemical properties of the serum supplement. In Vitro 18:576–584. [PubMed: 7118138]

Ries C, Egea V, Karow M, Kolb H, Jochum M, Neth P. 2007 MMP-2, MT1-MMP, and TIMP-2 are essential for the invasive capacity of human mesenchymal stem cells: differential regulation by inflammatory cytokines. Blood 109:4055–63. [PubMed: 17197427]

Ross AE, Tang MY, Gemeinhart RA. 2012 Effects of Molecular Weight and Loading on Matrix Metalloproteinase-2 Mediated Release from Poly(Ethylene Glycol) Diacrylate Hydrogels. Aaps Journal 14:482–490. [PubMed: 22535508]

Sakamoto N, Tsuji K, Muul LM, Lawler AM, Petricoin EF, Candotti F, Metcalf JA, Tavel JA, Lane HC, Urba WJ, Fox BA, Varki A, Lunney JK, Rosenberg AS. 2007 Bovine apolipoprotein B-100 is a dominant immunogen in therapeutic cell populations cultured in fetal calf serum in mice and humans. Blood 110:501. [PubMed: 17395779]

Shih YRV, Tseng KF, Lai HY, Lin CH, Lee OK. 2011 Matrix Stiffness Regulation of Integrin-Mediated Mechanotransduction During Osteogenic Differentiation of Human Mesenchymal Stem Cells. Journal of Bone and Mineral Research 26:730–738. [PubMed: 20939067]

Silva Paiva KB, Granjeiro JM. 2014 Bone tissue remodeling and development: Focus on matrix metalloproteinase functions. Archives of Biochemistry and Biophysics 561:74–87. [PubMed: 25157440]

Steinmetz NJ, Bryant SJ. 2011 The effects of intermittent dynamic loading on chondrogenic and osteogenic differentiation of human marrow stromal cells encapsulated in RGD-modified poly(ethylene glycol) hydrogels. Acta Biomaterialia 7:3829–3840. [PubMed: 21742067]

Tibbitt MW, Anseth KS. 2009 Hydrogels as Extracellular Matrix Mimics for 3D Cell Culture. Biotechnology And Bioengineering 103:655–663. [PubMed: 19472329]

Turk BE, Huang LL, Piro ET, Cantley LC. 2001 Determination of protease cleavage site motifs using mixture-based oriented peptide libraries. Nature Biotechnology 19:661–667.

Vincenti MP, White LA, Schroen DJ, Benbow U, Brinckerhoff CE. 1996 Regulating expression of the gene for matrix metalloproteinase-1 (collagenase): Mechanisms that control enzyme activity, transcription, and mRNA stability. Crit. Rev. Eukaryot. Gene Expr. 6:391–411. [PubMed: 8959374]

Wang X, Hu X, Dulinska-Molak I, Kawazoe N, Yang Y, Chen G. 2016 Discriminating the Independent Influence of Cell Adhesion and Spreading Area on Stem Cell Fate Determination Using Micropatterned Surfaces. Scientific Reports 6:28708. [PubMed: 27349298]

Wang YK, Yu X, Cohen DM, Wozniak MA, Yang MT, Gao L, Eyckmans J, Chen CS. 2012 Bone morphogenetic protein-2-induced signaling and osteogenesis is regulated by cell shape, RhoA/ROCK, and cytoskeletal tension. Stem cells and development 21:1176–86. [PubMed: 21967638]

You L-D, Weinbaum S, Cowin SC, Schaffler MB. 2004 Ultrastructure of the osteocyte process and its pericellular matrix. Anat Rec A Discov Mol Cell Evol Biol 278:505–513. [PubMed: 15164337]

Zhang T, Lin S, Shao X, Zhang Q, Xue C, Zhang S, Lin Y, Zhu B, Cai X. 2017 Effect of matrix stiffness on osteoblast functionalization. Cell Prolif 50.

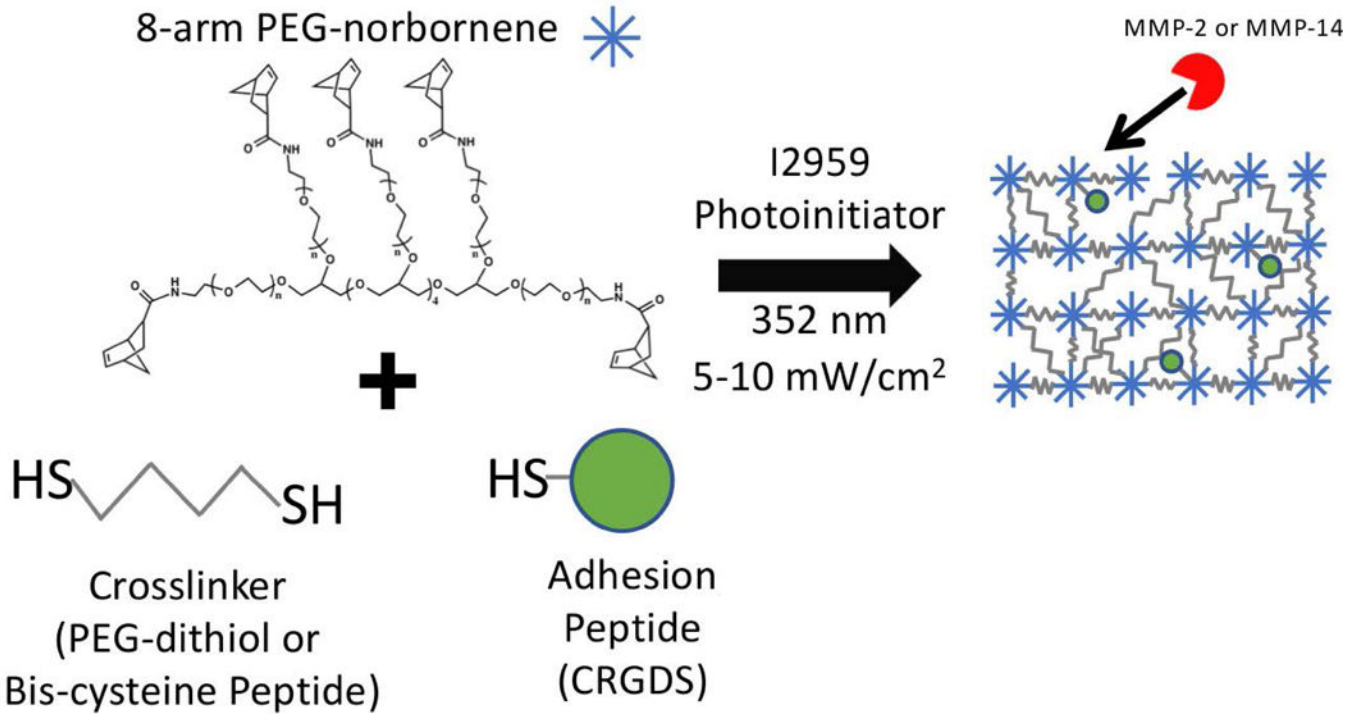

Figure 1.

Schematic diagram depicting the photopolymerization of 8-arm PEG functionalized with norbornene macromers, CRGDS, and crosslinker molecules to form PEG hydrogels with non-degradable crosslinks (PEG-dithiol) or with MMP-sensitive peptide crosslinks.

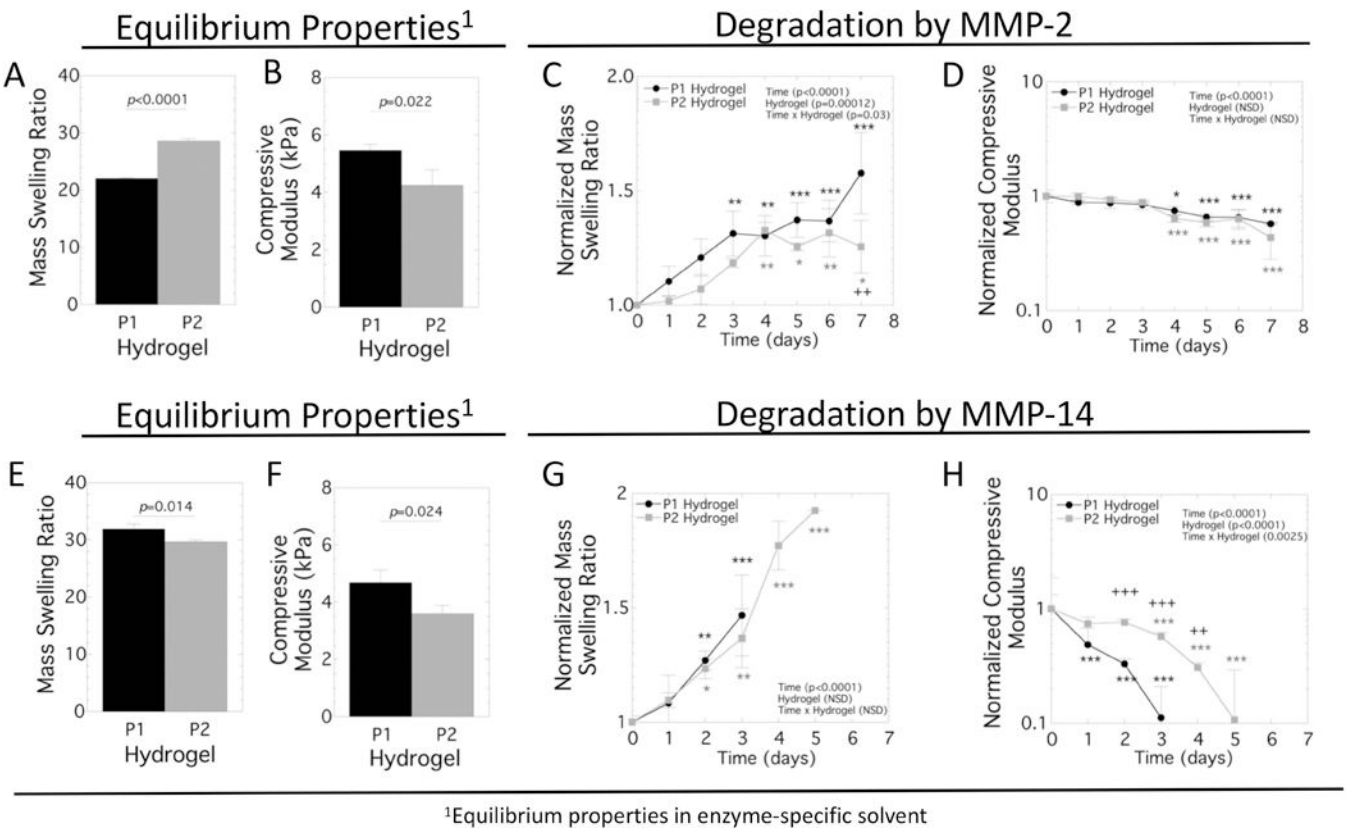

Figure 2.

Characterization of the acellular MMP-sensitive hydrogels formed with the P1 and P2 crosslinkers. The equilibrium hydrogel properties were initially measured in the swelling solvent appropriate for enzyme (see materials and methods) after 48 hours and then measured as a function of time in the presence of enzyme, with time 0 days indicating when the enzyme was introduced. For MMP-2, the equilibrium properties prior to exposure to enzyme are shown for A) mass swelling ratio and B) compressive modulus. In the presence of MMP-2, C) mass swelling ratio normalized to the equilibrium mass swelling ratio and D) compressive modulus normalized to the equilibrium compressive modulus are reported as a function of time. For MMP-14, the equilibrium properties prior to exposure to enzyme are shown for E) mass swelling ratio and F) compressive modulus. In the presence of MMP-14, C) mass swelling ratio normalized to the equilibrium mass swelling ratio and D) compressive modulus normalized to the equilibrium compressive modulus are reported as a function of time. The enzyme concentrations were 0.5 nM MMP-2 or 1.5 nM MMP-14. P1 hydrogel is shown in black in the bar graphs or with black circles in the line plots. P2 hydrogel is shown in gray in the bar graphs or with gray squares in the line plots. Data are shown as mean with standard deviation as error bars (n=3). A two-way fixed ANOVA was performed and *p*-values are reported for the main effects of time and hydrogel and their interaction. The asterisks at a given time point indicate significant differences from the initial time point (* $p<0.05$, ** $p<0.01$, and *** $p<0.001$) with the black and gray correlating to P1 and P2 hydrogels, respectively. The $^{+}$ symbol indicates significance difference between the P1 and P2 hydrogels ($^{++}$ $p<0.01$ and $^{+++}$ $p<0.001$).

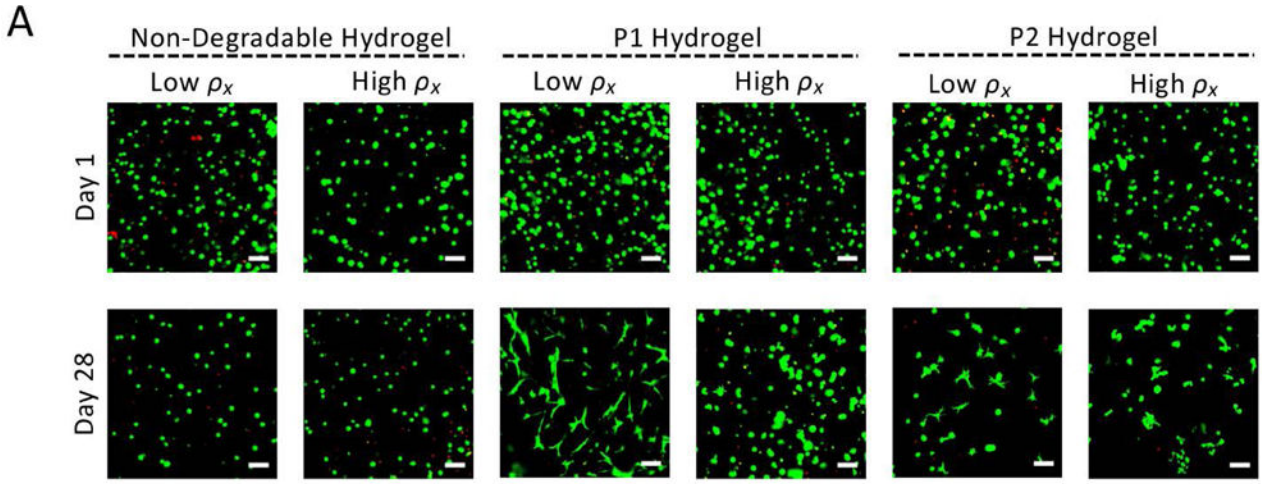

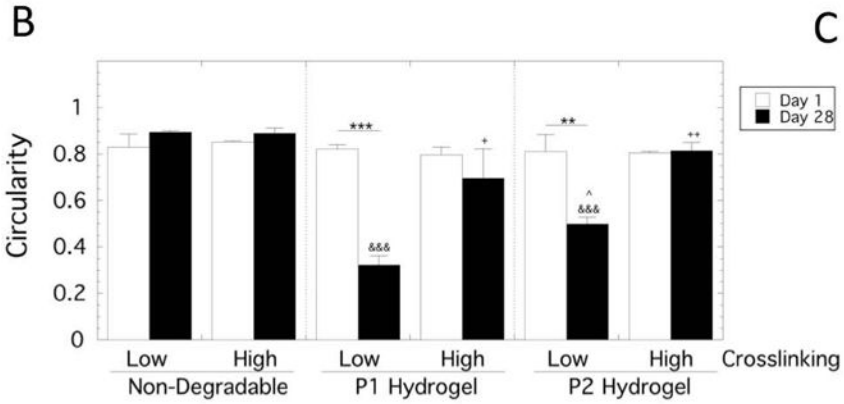

C

Main Effect	Factor	P-value
Non-degradable	Time	NSD
	Crosslinking	NSD
	Interaction	NSD
P1 Hydrogel	Time	0.004
	Crosslinking	0.024
	Interaction	0.016
P2 Hydrogel	Time	0.008
	Crosslinking	0.008
	Interaction	0.007
Low Crosslinking	Time	<0.001
	Hydrogel Type	<0.001
	Interaction	<0.001
High Crosslinking	Time	NSD
	Hydrogel Type	NSD
	Interaction	NSD

Figure 3.

Assessment of viability and cell shape of hMSCs encapsulated and cultured in non-degradable, P1 and P2 PEG hydrogels of low and high crosslinking density. A) Representative confocal microscopy images depicting live, stained by Calcein AM (green), and dead, stained by ethidium homodimer (red). Scale bar is 100 μm. B) Cell shape was measured by circularity from the confocal microscopy images for live cells. Data are presented as mean with standard deviation as error bars (n=2). Statistical significance from pairwise comparisons are shown where * symbol indicates significance between two time points given by the bar, & symbol indicates significance with non-degradable hydrogel at the same crosslinking density, and ^ symbol indicates significance with P1 hydrogel of the same crosslinking density, and + symbol indicates significance with the low crosslinking density of same hydrogel type. One symbol indicates $p<0.05$, two symbols indicate $p<0.01$, three symbols indicate $p<0.001$. C) Statistical analysis results for cellularity. A three-way ANOVA with hydrogel type, hydrogel crosslink density, and culture time revealed a significant three-way interaction. Therefore, select two-way ANOVAs were and the results are provided.

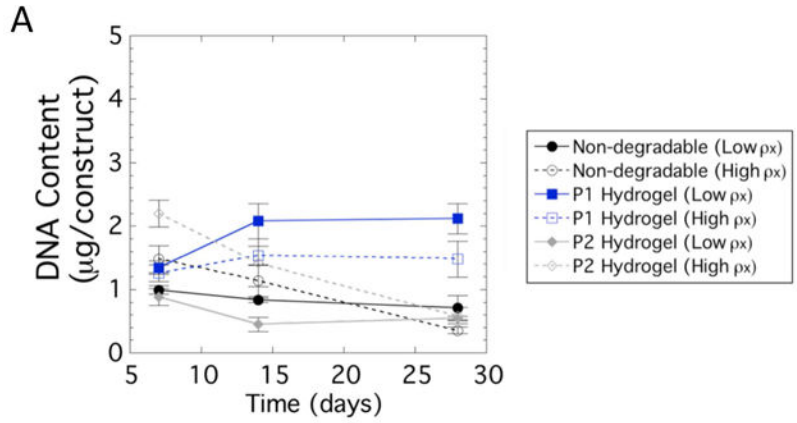

B

Main Effect	Factor	P-value
Non-degradable	Time	<0.001
	Crosslinking	NSD
	Interaction	<0.001
P1 Hydrogel	Time	0.002
	Crosslinking	0.001
	Interaction	NSD
P2 Hydrogel	Time	<0.001
	Crosslinking	<0.001
	Interaction	<0.001

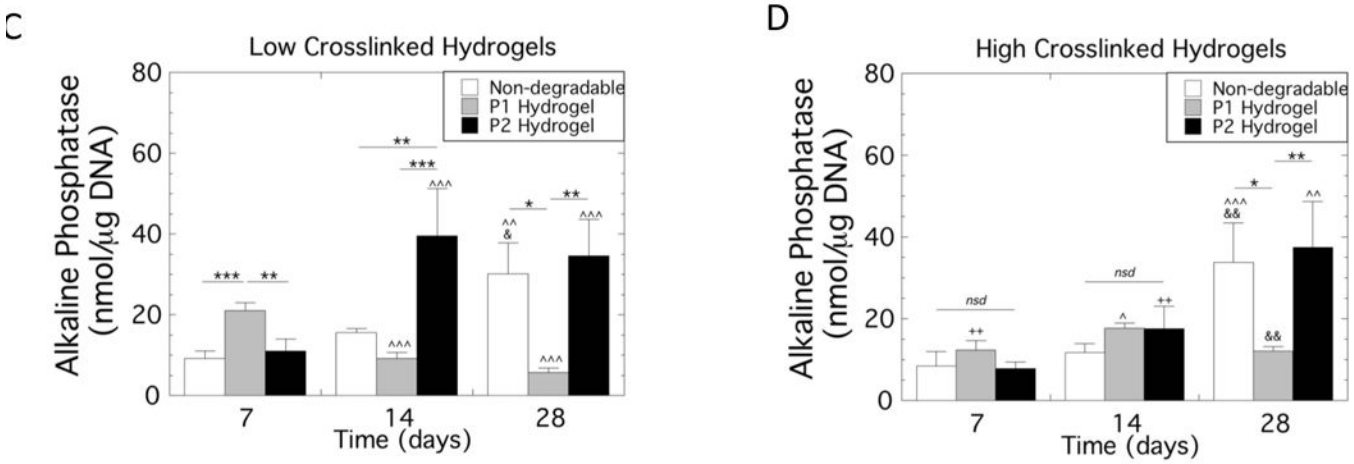

E

Main Effect	Factor	P-value
Day 7	Hydrogel Type	<0.001
	Crosslinking	0.004
	Interaction	0.044
Day 14	Hydrogel Type	<0.001
	Crosslinking	0.045
	Interaction	0.001
Day 28	Hydrogel Type	<0.001
	Crosslinking	NSD
	Interaction	NSD

Main Effect	Factor	P-value
Non-degradable	Time	<0.001
	Crosslinking	NSD
	Interaction	NSD
P1 Hydrogel	Time	<0.001
	Crosslinking	0.02
	Interaction	<0.001
P2 Hydrogel	Time	<0.001
	Crosslinking	NSD
	Interaction	NSD

Figure 4.

DNA content and Alkaline phosphatase activity (ALP) by hMSCs encapsulated and cultured in non-degradable, P1 and P2 PEG hydrogels of low and high crosslinking density. A) Double stranded DNA content. B) Statistical analysis results of DNA content. A three-way ANOVA with hydrogel type, hydrogel crosslink density, and culture time revealed a significant three-way interaction. Therefore, two-way ANOVAs were performed holding each main effect for hydrogel type and crosslinking constant and the results are provided. C) ALP activity normalized to DNA content as a function of time for the low crosslinked hydrogels. D) ALP activity normalized to DNA content as a function of time for the high crosslinked hydrogels. Data are presented as mean with standard deviation as error bars (n=3). E) Statistical analysis results of ALP activity. A three-way ANOVA with hydrogel type, hydrogel crosslink density, and culture time revealed a significant three-way

interaction. Therefore, select two-way ANOVAs were performed and the results are provided. Statistical significance from pairwise comparisons are shown where * symbol indicates pairwise significance defined by the bar, ^ symbol indicates significance with day 7 of the same crosslinking density and hydrogel, & symbol indicates significance with day 14 of the same crosslink density and hydrogel, and + symbol indicates significance with the low crosslinking density of same hydrogel type. One symbol indicates $p<0.05$, two symbols indicate $p<0.01$, three symbols indicate $p<0.001$.

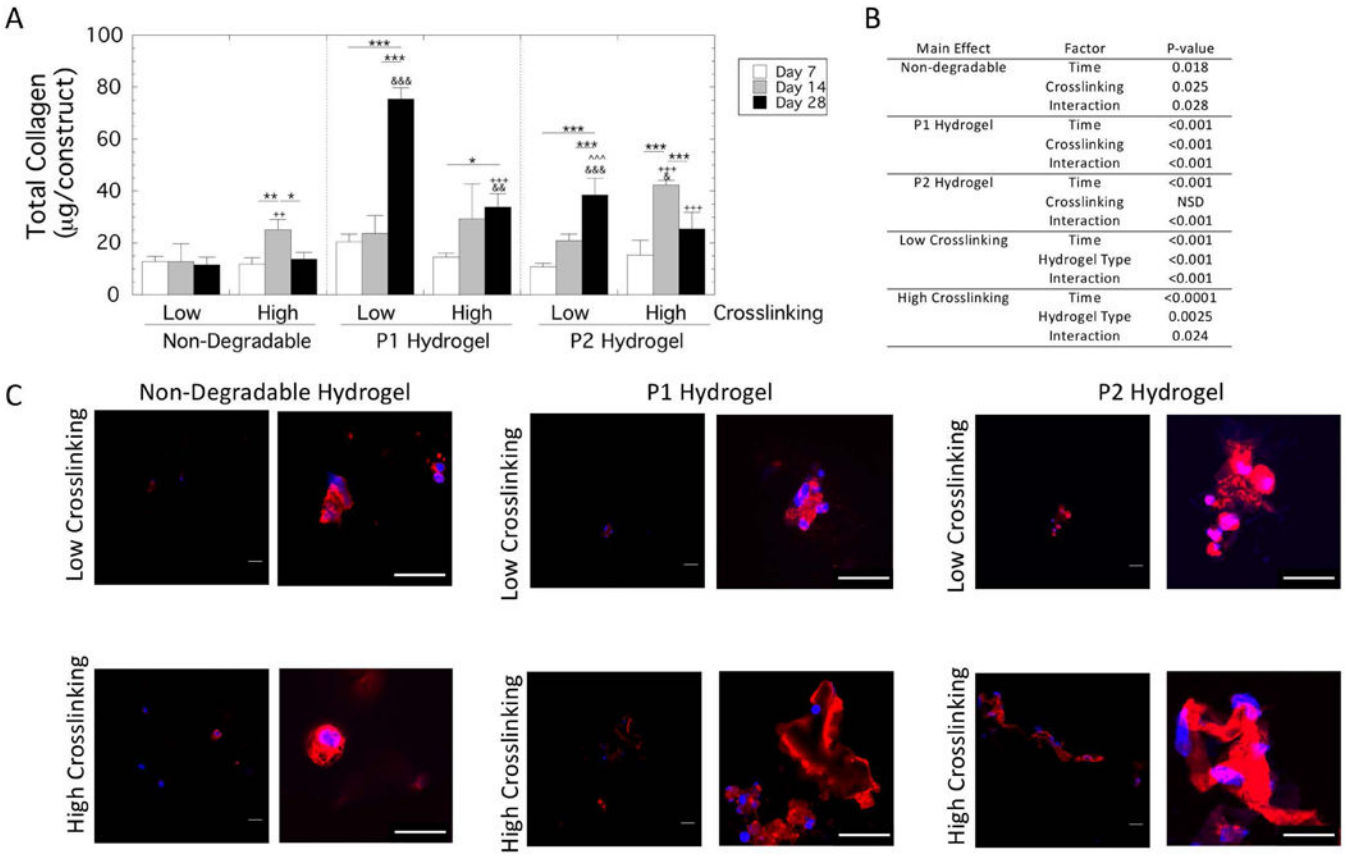

Figure 5.

Total collagen content by hMSCs encapsulated and cultured in non-degradable, P1 and P2 PEG hydrogels of low and high crosslinking density. A) Total collagen content per construct at days 7, 14 and 28. Data are presented as mean with standard deviation as error bars (n=3) Statistical significance from pairwise comparisons are shown where * symbol indicates significance between two time points given by the bar, & symbol indicates significance with non-degradable hydrogel at the same crosslinking density, and ^ symbol indicates significance with P1 hydrogel of the same crosslinking density, and + symbol indicates significance with the low crosslinking density of same hydrogel type. One symbol indicates $p<0.05$, two symbols indicate $p<0.01$, three symbols indicate $p<0.001$. B) Statistical analysis results. A three-way ANOVA with hydrogel type, hydrogel crosslink density, and culture time revealed a significant three-way interaction. Therefore, select two-way ANOVAs were performed and the results are provided. C) Representative confocal microscopy images of sections stained for collagen type I (red) and counterstained with Dapi (blue) are shown for day 28. A higher magnification view is provided by the image to the right to assist in visualizing the localized collagen I deposition. Scale bar is 20 µm.

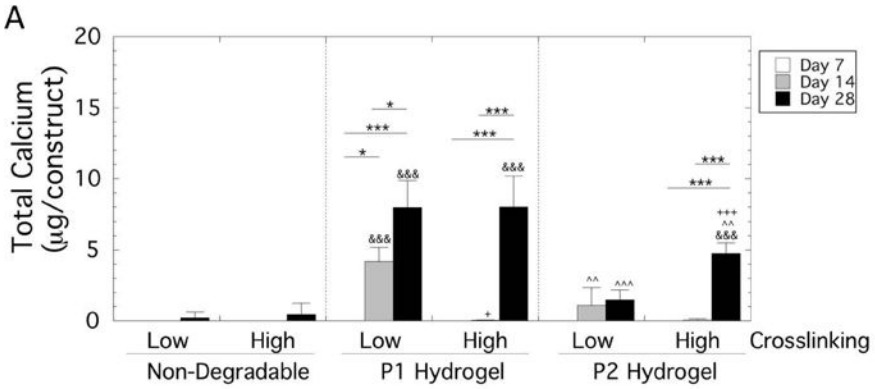

B

Main Effect	Factor	P-value
Non-degradable	Time	NSD
	Crosslinking	NSD
	Interaction	NSD
P1 Hydrogel	Time	<0.001
	Crosslinking	0.039
	Interaction	0.02
P2 Hydrogel	Time	<0.001
	Crosslinking	0.034
	Interaction	<0.001
Low Crosslinking	Time	<0.001
	Hydrogel Type	<0.001
	Interaction	<0.001
High Crosslinking	Time	<0.001
	Hydrogel Type	<0.001
	Interaction	<0.001

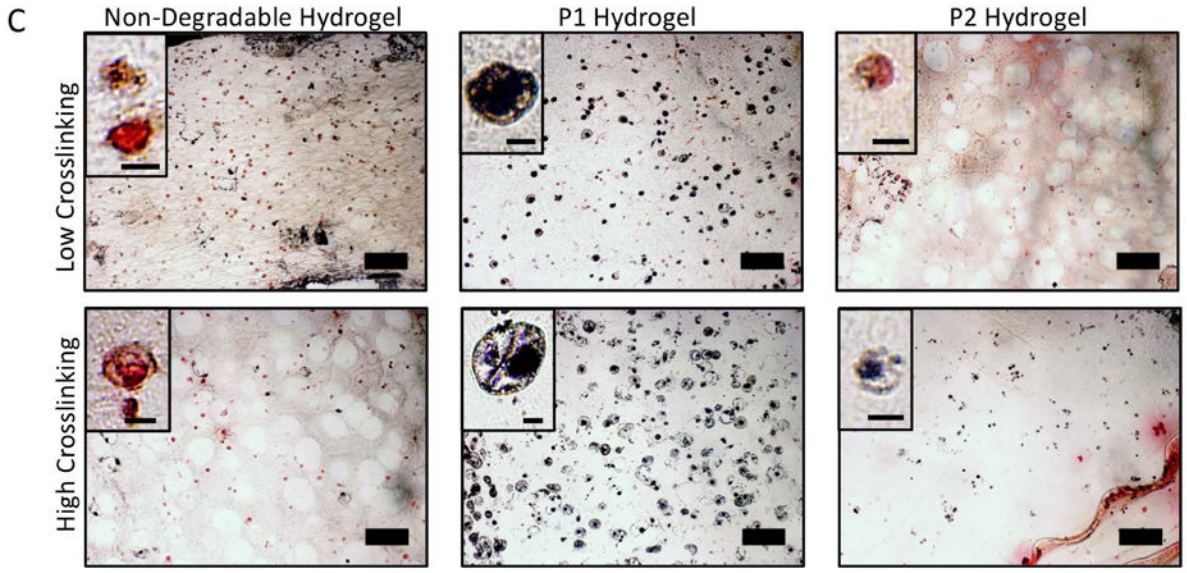

Figure 6.

Total calcium content by hMSCs encapsulated and cultured in non-degradable, P1 and P2 PEG hydrogels of low and high crosslinking density. A) Total calcium content per construct at days 7, 14 and 28. Data are presented as mean with standard deviation as error bars (n=3) Statistical significance from pairwise comparisons are shown where * symbol indicates significance between two time points given by the bar, & symbol indicates significance with non-degradable hydrogel at the same crosslinking density, and ^ symbol indicates significance with P1 hydrogel of the same crosslinking density, and + symbol indicates significance with the low crosslinking density of same hydrogel type. One symbol indicates $p<0.05$, two symbols indicate $p<0.01$, three symbols indicate $p<0.001$. B) Statistical analysis results. A three-way ANOVA with hydrogel type, hydrogel crosslink density, and culture time revealed a significant three-way interaction. Therefore, select two-way ANOVAs were performed and the results are provided. C) Representative microscopy images of sections stained for von Kossa and counterstained with nuclear red, where mineral deposits stain black, are shown for day 28. Scale bar is 100 µm. Inset shows a representative close-up of a cell with a scale bar of 10 µm.

A

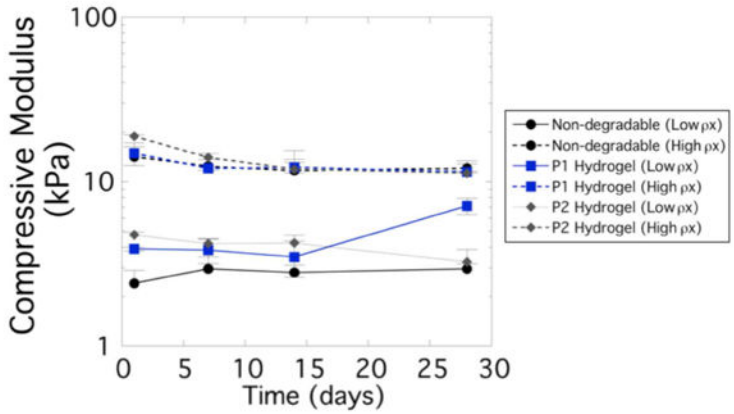

B

Main Effect	Factor	P-value
Non-degradable	Time	NSD
	Crosslinking	<0.001
	Interaction	NSD
P1 Hydrogel	Time	0.02
	Crosslinking	<0.001
	Interaction	<0.001
P2 Hydrogel	Time	NSD
	Crosslinking	<0.001
	Interaction	NSD
Low Crosslinking	Time	0.004
	Hydrogel Type	<0.001
	Interaction	<0.001
High Crosslinking	Time	0.009
	Hydrogel Type	NSD
	Interaction	NSD

Figure 7.

Compressive modulus of cell-laden hydrogel constructs for non-degradable hydrogels (black, circle), P1 hydrogels (blue, squares) and P2 hydrogels (diamond, dark gray) of low crosslink density (solid line) and high crosslink density (dotted line). A) Data are presented as mean with standard deviation as error bars (n=3). B) Statistical analysis results. A three-way ANOVA with hydrogel type, hydrogel crosslink density, and culture time revealed significant two-way interaction for each main effect. Therefore, select two-way ANOVAs were performed and the results are provided.

Table 1.

Hydrogel formulations used in this study

Hydrogel Type	Crosslinker	Ref	Thiol-ene Ratio	Low crosslinking (w/w PEG-NB)	High crosslinking (w/w PEG-NB)
P1	CVPLS-LYSGC	(Turk et al., 2001)	0.8	3 %	6 %
P2	CRGRIGF-LRTDC	(Kridel et al., 2002)	0.8	3 %	6 %
Non-degradable	PEG dithiol	N/A	0.6	3 %	6 %